

Published: September 30, 2023

Citation: Yannas, V. I., 2023. Contraction blocking during wound healing of three injured organs leads to absence of scar and induction of regeneration. Medical Research Archives, [online] 11(9). <https://doi.org/10.18103/mra.v11i9.4471>

Copyright: © 2023 European Society of Medicine. This is an open-access article distributed under the terms of the Creative Commons Attribution License, which permits unrestricted use, distribution, and reproduction in any medium, provided the original author and source are credited.

DOI: <https://doi.org/10.18103/mra.v11i9.4471>

ISSN: 2375-1924

RESEARCH ARTICLE

Contraction blocking during wound healing of three injured organs leads to absence of scar and induction of regeneration

Ioannis V. Yannas

Massachusetts Institute of Technology, Cambridge MA, USA

yannas@mit.edu

ABSTRACT

We report the central role of mechanical contraction in healing of wounds in animal models, as well as in humans. Our evidence has been collected from studies of excised skin wounds as well as with the transected peripheral nerve and the excised conjunctiva. We have observed that, following blocking of contraction, wounds in our animal models close by regeneration of the injured tissues. We review the mechanism of contraction blocking and tissue regeneration when wounds are grafted with a highly porous Type I collagen scaffold, named dermis regeneration template (DRT) which is required for inducing regeneration.

Introduction

During healing wounds contract from the mechanical action of differentiated fibroblasts known as myofibroblasts (MFB). MFB pull the edges of the wound together and wound closure is eventually achieved by synthesis of scar which appears to act as a sealant that securely keeps the wound edges closed.

The process of wound contraction is of special interest after observing that blocking of contraction by a highly porous scaffold, dermis regeneration template (DRT), has been followed by regeneration of excised skin, transected nerve and excised conjunctiva in animal models. In this review we examine the process by which blocking of wound contraction leads to regeneration of the injured tissues.

A. PHYSIOLOGY OF WOUND CLOSURE:

The focus of this chapter is primarily on wound closure. Exactly how wounds close anywhere in the body determines whether the wound has closed by repair or regeneration. Repair heals the interrupted continuity of tissues by contraction of the wound perimeter and synthesis of scar without restoration of the physiological tissues. Regeneration, in contrast, heals by synthesis of the missing tissues at the original anatomic site, yielding a regenerate, not scar. Regeneration restores the normal structure and function of the injured tissues; repair does not.

Determination of the outcome of a healing process as either repair or regeneration can be made using an experimental protocol that is based on the concept of an *anatomically well-defined wound*¹. Since the outcome of an injury depends critically on the precise nature of the injury itself it is necessary to limit the

study of regeneration to the type of wound that is both standardized and appropriate to the purpose of such a study. In a study of regeneration of skin, for example, it is required to eliminate from the wound traces of the native dermis before proceeding with the study: For an obvious example, an experimental study of dermis regeneration that includes leftover dermis at the experimental site would not be expected to provide an acceptable test of its objective.

A clear distinction among three types of tissues in individual organs can be made in terms of their ability to regenerate spontaneously. This "tissue triad"¹ comprises epithelia, basement membrane and stroma. In general, epithelia cover all body surfaces and are separated from stroma by a contiguous basement membrane. Epithelia comprise cells but no extracellular matrix (ECM) and are not penetrated by blood vessels, the basement membrane (BM) comprises components of ECM but no cells and has no blood vessels and the stroma comprises cells, ECM and blood vessels as well. In skin the epidermis is the epithelial tissue and the basement membrane separates the epidermis from the dermis (stroma). In peripheral nerves the myelin sheath is the epithelial tissue and the BM separates it from the endoneurial stroma. Epithelial tissue regenerates spontaneously and so does the associated basement membrane; however, the stroma does not regenerate spontaneously. Since the stroma is the tissue that is incapable of spontaneous regeneration we regard stroma regeneration as the central problem in the science of regeneration¹.

As examples of these basic principles we refer to the injury responses in skin and peripheral

nerve, two organs that have been studied assiduously by clinical investigators. Healing in these two organs is the experimental paradigm that we will employ in this chapter. It has been observed in skin and peripheral nerve studies that an injury that perforates the epithelial tissue alone (epidermis in skin, myelin sheath in nerves) but not the basement membrane is reversible, leading to regeneration. In contrast, perforation of stroma (dermis in skin, endoneurial stroma in nerves) sets off the classical wound healing response which is an irreversible process leading to scar formation¹. Finally, the requirement in this chapter for citing evidence solely from anatomically well-defined wounds is met by selecting the three injuries featured below: full-thickness excision of the skin

(guinea pig), transection of the rat sciatic nerve (rat) and excision of the conjunctival stroma (rabbit).

A closed wound in excised guinea pig skin (Fig 1) illustrates the process of wound closure by highlighting contraction, which brings the dermal edges close together, and scar formation, which appears to seal the wound edges securely. There is striking evidence of tissue deformation of subdermal tissue due to mechanical forces associated with the contraction process. There is no restoration of physiological tissue. Fig 1 provides an example of wound closure by repair.

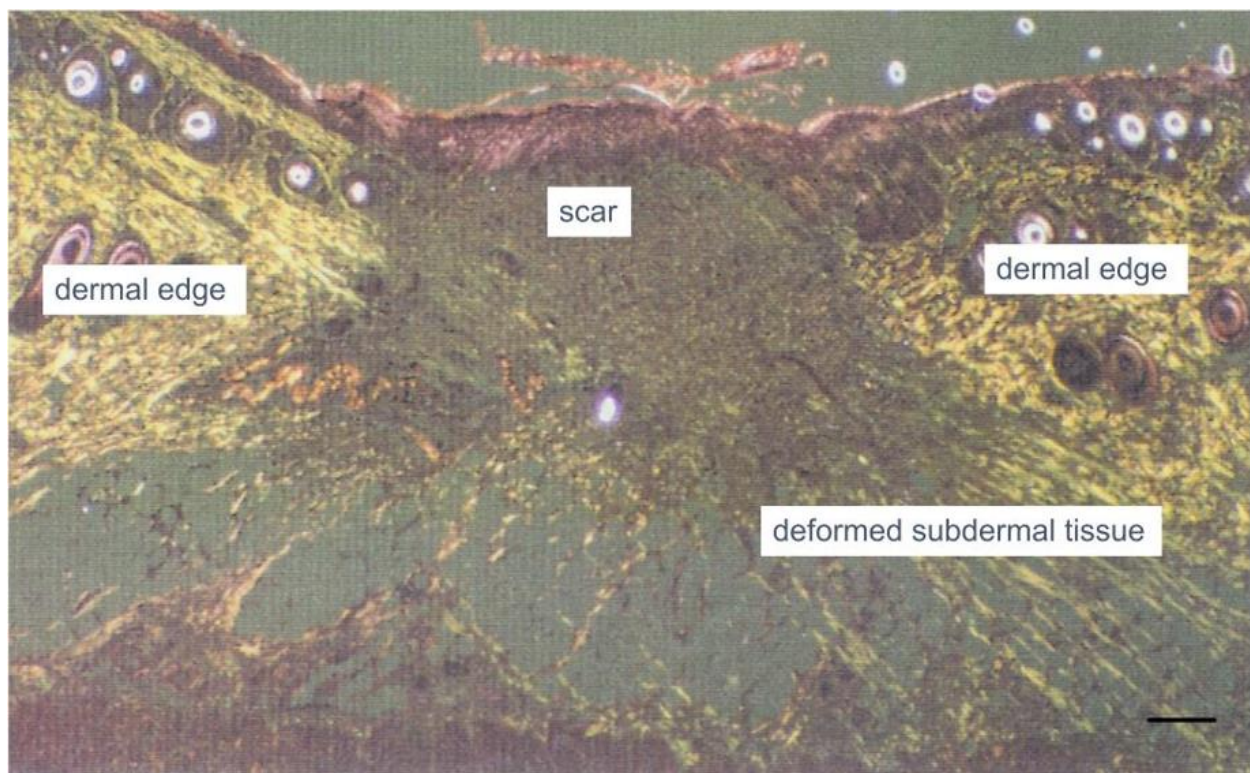


Fig. 1. Physiological closure of an excisional full-thickness skin wound in the guinea pig¹. Observed by polarized light microscopy. *Left, right*: Following contraction the dermal edges are separated by scar. *Top center*: Scar. *Bottom right*: Highly deformed birefringent fibers (probably stretched collagen fibers) underneath scar. *Scale bar*: 100 μ m. (from K.Troxel)

B. WOUND CONTRACTION BY MYOFIBROBLASTS IS LARGELY BLOCKED BY DRT:

Wound closure in mammals is generally shared by three distinct processes: Contraction, scar formation and regeneration. Physiological healing consists of the first two processes; regeneration lies dormant in adult mammals and requires specific activation².

An experimental description of wound healing processes in mammals, including wound closure either by repair or regeneration, appears in Fig. 2 for three animal models: excised skin (guinea pig), transected peripheral nerve (rat) and the excised conjunctiva (rabbit)². Detailed references to the original data appear in Fig. 2².

The **left panel** of Fig. 2 presents the macroscopic view of the injury inflicted in each animal model. Individual animal models of injury are identified by the letters **a, f, k** in Fig. 2. The **central panel** of Fig. 2, labelled "MFB Assembly" (myofibroblast assembly), provides a view of the immunohistochemical description of the wound healing process several days after injury (10 days after skin excision, 7 days after nerve transection, 14 days after conjunctival injury); individual photos are identified by letters **b, d, g, i, l** and **n**. Myofibroblasts (MFB) are stained for alpha smooth muscle actin (*red brown in skin and conjunctiva wounds, brown in nerve wounds*). The **right panel** of Fig. 2 presents the long term outcome of the healing process. Individual photos are identified by the letters **c, e, h, j, m, o**. For each of the animal models in Fig. 2 the photos displayed in the central (short term) and right panels (long term) provide information about the effect of treatment: either untreated (No DRT) or

grafted with DRT (dermis regeneration template, a highly porous collagen-based scaffold¹).

In the absence of DRT treatment the photos in the central panel of Fig. 2 describe physiological wound contraction in the three injured animal models (photos labeled **b, g, l**). Contraction of skin (**b**) and nerve wounds (**g**) features a dense MFB population, extensive MFB clustering and high orientation of MFB long axes along a major direction; these effects are present but less evident in conjunctival wounds (**l**). In skin wounds and conjunctiva wounds, the stroma is largely planar and the major axis for MFB orientation is likewise located in the plane of the wound; MFB eventually close the skin wound by applying tensile forces in the plane of the wound. A similar arrangement is in effect in the planar conjunctival wound. In peripheral nerve wounds the MFB (*brown*) are wrapped around the cylindrical neural tissue in a circumferential orientation.

The dramatic effect on wound contraction following grafting with DRT is illustrated in the central panel of Fig. 2 (photos **d, i, n**). All three features of physiological contraction are altered in the presence of DRT: The MFB density is reduced, MFB clustering is strikingly unraveled and MFB axial orientation is lost. Since MFB provide the only engine that applies tensile forces inward at the wound edges to achieve wound closure we conclude that these changes resulting from DRT grafting denote a substantial loss in macroscopic contractile activity. Indeed it is observed in animal studies that grafting with DRT arrests the physiological contraction process in skin wounds.

C. SCAR FORMATION BY MYOFIBROBLASTS IS PREVENTED BY CONTRACTION BLOCKING: Synthesis of scar appears to occur when, during the process of wound contraction, MFB become involved in a dynamic exchange of phenotypes, primarily including contractile and synthetic phenotypes³. The synthetic phenotypes (mostly synthesis of collagen fibers) appear to dominate as the mechanical stiffness of the substrate increases³. In independent studies of collagen synthesis, it has been shown that the axis of a newly synthesized collagen fiber is aligned with the axial orientation of the parent fibroblast⁴. In the contractile mechanical field of the healing wound, myofibroblasts are forced to adopt an oriented configuration along the major deformation axis (Fig. 2, b). It is expected therefore that newly synthesized collagen fibers that constitute scar would also possess high orientation along a similar wound axis as do the parent cells, as indeed observed by laser light scattering of collagen fibers in dermal scar⁵. On a larger scale we have further observed that oriented collagen fibers were formed on the plane of the skin wound; in peripheral nerves, fibers were formed circumferentially around the transected nerve¹. We conclude that scar deposition in these models adapted to the physiological anatomic topography of the individual organ.

The long term outcome of the healing processes for the three animal models of injury is illustrated in the **right panel** of Fig. 2. In full-thickness skin wounds, birefringence microscopy of collagen fibers in DRT-ungrafted wounds contrasts the formation of fibers that are highly oriented in the plane characterizing scar (c) with synthesis of quasi randomly oriented collagen fibers in the nearly-

physiological dermis of DRT-grafted wounds (e). In DRT-ungrafted peripheral nerve wounds (h) electron microscopy reveals that, 26 months following nerve transection, the original nerve fibers have been replaced by a dense sheaf of collagen fibrils that enclose groups of Schwann cells (Büngner bands, Bb). In contrast (j), histological micrographs of cross sections from DRT-grafted peripheral nerves demonstrate the formation of neural tissue exhibiting histomorphometric (equivalent diameter, number of myelinated fibers, number of A-fibers) and electrophysiological assay results that were similar to those for the autograft. In conjunctival wounds, immunohistochemical analysis and birefringence microscopy demonstrate scar formation in DRT-ungrafted wounds (m, note marked orientation of collagen fibers characteristic of scar formation) and synthesis of near-normal conjunctival stroma collagen fibers (no significant fiber orientation) in DRT-grafted wounds (o).

In summary, the long term data in Fig. 2 show that, in all three animal models, grafting with DRT prevented scar formation and resulted in regenerated tissue in skin (e), nerve (j) and conjunctiva (o).

A simple explanation for the induced regeneration is blocking of wound contraction and scar formation by DRT grafting which immediately preceded regeneration. We attempt to identify below the mechanism of the blocking process.

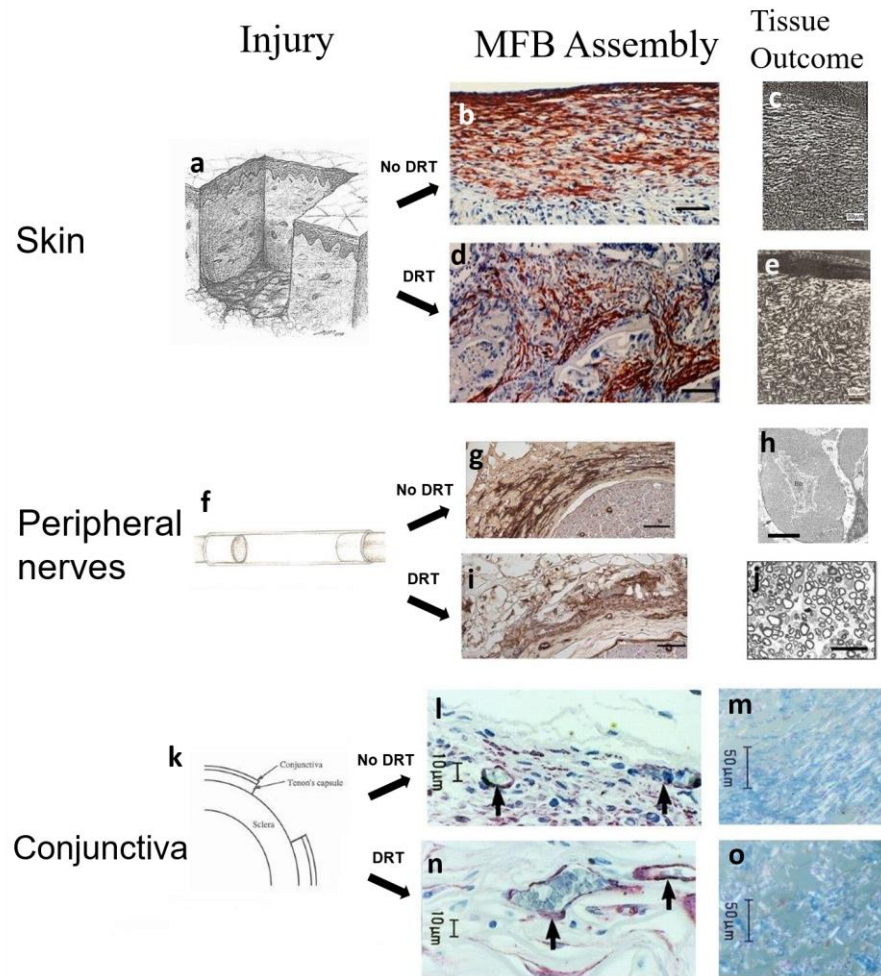


Fig. 2. Wound contraction and associated wound healing response in three models of adult injury viewed both in the absence (spontaneous healing) and presence of a DRT graft². *Left vertical panel*: Illustrates the experimental injury site in skin (*top*), peripheral nerve (*middle*) and conjunctiva (*bottom*). All injuries emphasize excision of the stroma. *Middle vertical panel*: Illustrates the early response of each animal model to the injury in the absence and presence of a DRT graft. Myofibroblasts (MFB) are stained (*red brown in skin and conjunctiva, brown in nerve*) with antibody to aSMA. MFB assemblies responded very strongly to DRT compared to DRT-free control, exhibiting lower density, disassembled clusters and loss in axial orientation. *Scale bars*: skin and nerves, 100 μm ; conjunctiva, 10 μm . *Right vertical panel*: Illustrates the long term effect of DRT grafting compared to DRT-free control. In DRT-free healing the outcome was scar, a collagen-based anisotropic tissue characterized by oriented fibers. In DRT-treated injuries the outcome was synthesis of physiological, or nearly physiological, stroma characterized by a relatively random arrangement of collagen fibers, distinct from scar. *Scale bars*: skin, 50 μm ; peripheral nerve, neural scar (top), 2 μm ; peripheral nerve, regenerated nerve (bottom), 25 μm ; conjunctiva, 50 μm .

D.SURFACE BIOLOGY OF THE INDUCED REGENERATION PROCESS:

An early study⁶ of the contraction-blocking activity of several DRT analogs differing in average pore diameter ("pore size") but identical in other structural features was conducted (Fig. 3). An increase in values along the y-axis

of Fig. 3 indicates increase in contraction blocking. The data illustrate the intriguing observation that the contraction blocking activity was maximized when the pore size was in the range approximately 20 to 140 μm . The presence of this maximum eventually provided a clue to the origin of DRT contraction-

blocking activity. A scanning electron microscopic view of DRT is shown in Fig. 4.

The physics of porous materials provides a potential explanation for the observed maximum in terms of the natural variation of the specific surface (the entire surface area of the porous structure expressed in mm^2/mm^3) with the average pore size of the material. At constant pore volume fraction (percent pore volume for the entire volume of the material) the specific surface varies inversely with the pore size. It follows that, at very large values of the pore size, the specific surface falls to very low values; the opposite is true at very small values of the pore size.

To explain the observed variations in contraction-blocking activity with pore size we will consider first the hypothetical loss of attachment of MFB cells to each other in favor of attachment to the DRT surface. We recall from Fig. 2 that attachment of MFB cells to other MFB cells drives wound contraction (b) while attachment of MFB to the DRT surface (d) diminishes (blocks) contraction. A specific molecular binding event involving MFB and DRT was previously demonstrated following a study by multiphoton microscopy⁷. On the strength of this evidence⁷ we suggest therefore that the observed increase in contraction blocking with pore size along the range 500 μm to 120 μm (Fig. 3) can be explained in terms of the hypothetical variation in number of MFB switching their attachment away from other MFB cells to an attachment to the DRT surface. We also note that when the pore size becomes much smaller than the rough value of the cell diameter, about 10 μm , cells would be excluded from entering scaffold pores; below that critical value of the pore size, MFB

attachment to DRT is cancelled out and the overall contraction blocking effect reaches zero, i.e., becomes equal to the effect observed with the ungrafted control (no DRT). (Fig. 5)

The presence of a maximum in contraction blocking shown in Fig. 3 is therefore explained by the opposing directions of the two processes: increasing blocking with decreasing pore size (corresponding to an increase in specific surface) and a sharp decrease in blocking at the very low pore size ($<10 \mu\text{m}$) where migration of cells into the scaffold pores is excluded due to the size effect. In summary, we are suggesting that the DRT surface competitively inhibits MFB-MFB binding, which drives contraction, in favor of MFB-DRT binding, which blocks contraction.

In summary, comparison of the extent of cell clustering inside each of these two scaffolds in Fig. 5 supports the hypothesis that wound contraction is blocked when MFB-MFB binding (Fig. 5 *left*) is replaced by MFB-DRT binding (Fig. 5 *right*).

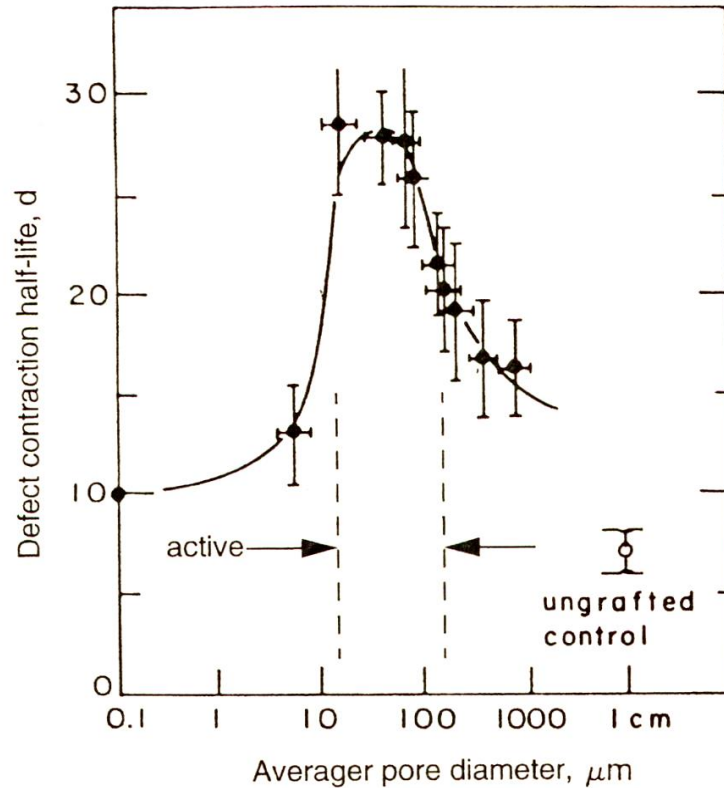


Fig. 3. The wound contraction-blocking activity of a large number of scaffolds that differ only in average pore diameter ("pore size") is plotted vs the pore size⁶. Contraction is inhibited maximally when the scaffold pore diameter is in the range 20 — 120 μm. The horizontal axis is logarithmic to accommodate the wide range in pore size in this study.

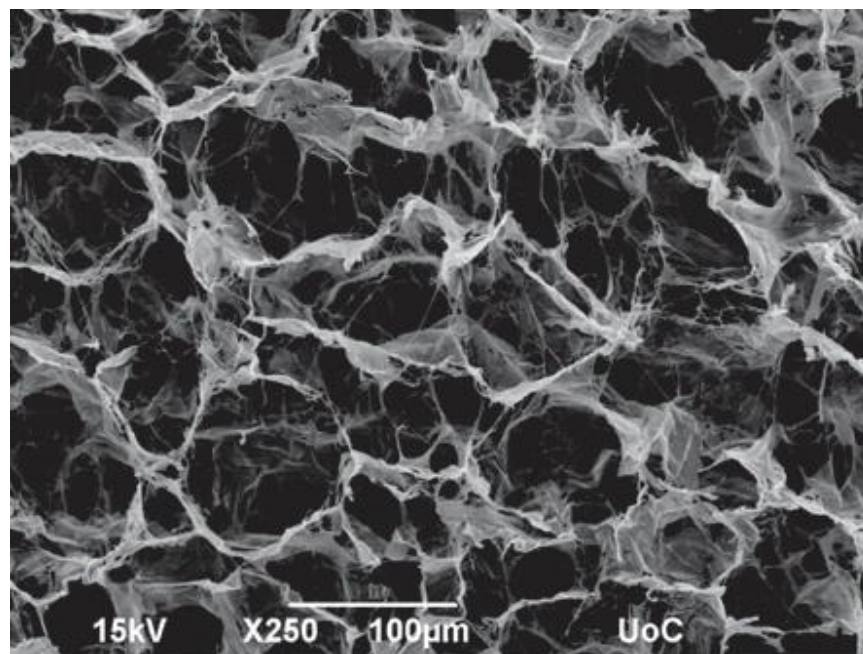


Fig. 4. A scanning electron microscopic view of the dermis regeneration template (DRT). The open pore structure is produced by freeze-drying under carefully controlled conditions a suspension of type I collagen-glycosaminoglycan block copolymer (photo by A. Kourgiantaki).

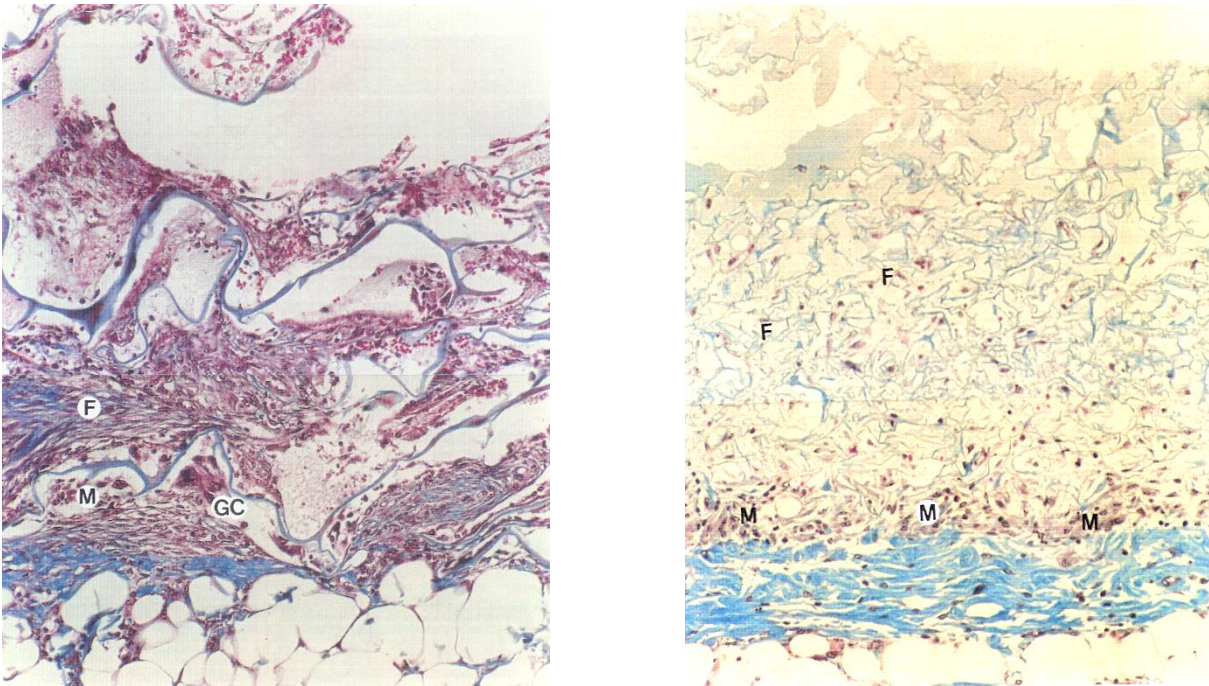


Fig. 5. Fibroblasts (*F*, red brown; not stained for *αSMA*) shown inside two collagen-based scaffolds implanted at the center of an excised skin wound in the guinea pig, day 7¹. *Left*: Fibroblasts form large, dense clusters (ca. 30-50 cells per cluster) inside the large pores of a scaffold with low regenerative activity, pore size 400 μm , specific surface ca. 2,000 mm^2/mm^3 . *Right*: Fibroblasts viewed inside a regeneratively active DRT analog, with average pore size 40 μm and much larger specific surface, ca.. 25,000 mm^2/mm^3 , appear isolated, forming small clusters (2-5 cells per cluster) inside the small pores. *M*, muscle boundary. *Arrows and GC*. Scaffold struts. *Scale bars*: 100 μm .

E. CLINICAL APPLICATIONS OF INDUCED REGENERATION IN PATIENTS:

The definitive effect of DRT in skin wound healing in animal models has introduced applications in a number of clinical areas where there is need to replace skin loss due to trauma or to replace skin that has an aesthetic defect. The early use of DRT⁸ was the post-excisional treatment of deep-partial to full-thickness burns where autograft supply was limited. These wounds had been excised down to muscle fascia early following injury⁹. Clinical studies of DRT (commercial name Integra[®]) with burn patients repeatedly showed synthesis of dermis in full-thickness wounds^{8,10}. Since DRT induces regeneration of the dermis, rather than the epidermis, it has been necessary to cover the newly synthesized dermis with an epidermal layer. With massively

burnt patients, rather than waiting for the much slower epidermal migration from the edges of the wound to cover the large-area wounds, the neodermal area was covered with a thin, autologous epidermal graft, largely free of dermis and measuring about 0.10-0.15 mm in thickness within a few weeks after grafting^{8,10}. Detailed histological studies of biopsies from the second clinical study¹⁰ showed that DRT fibers gradually disappeared, newly synthesized fibers became more coarse, and a distinction between papillary and reticular layers of the dermis appeared in the tissue layer of the dermis.

Although the early use of DRT was treatment of deep burns^{8,10}, over the years its use has expanded to reconstructive surgery and several other clinical areas¹¹. Examples are use

of Integra® to excise congenital nevi and grafting the excised area with DRT that eventually regenerates into skin¹², grafting chronic wounds in diabetics¹³, treatments for skin tumors¹⁴, traumatic injuries that involve the junction between muscle and bone (degloving)¹⁵, scalp reconstruction in elderly patients¹⁶ and treatment of exposed tendon¹⁷. Integra has also been used to control excessive scar formation, known as fibrosis^{18,19}. Over 2000 clinical studies of Integra are described in the following website:

<https://pubmed.ncbi.nlm.nih.gov/?term=Integra>.

Conclusions.

Wound closure in mammals generally occurs by three distinct processes: Contraction, scar formation and regeneration. Blocking of contraction by the dermis regeneration template (DRT), a highly porous collagen-based scaffold, has been shown to lead to absence of scar formation and incidence of regeneration of injured tissues. These findings, observed in three organs, namely, skin, peripheral nerve and the conjunctiva, have been successfully applied clinically in several cases of skin loss.

Conflict of Interest Statement:

I.V.Yannas is one of the cofounders of Integra Life Sciences Ltd. in 1993. He currently owns no shares of Integra LS Ltd. nor does he have any other direct financial connection with Integra LS Ltd.

Funding Statement:

None

Acknowledgement Statement:

None

References:

1. Yannas I.V., *Tissue and Organ Regeneration in Adults*, 2nd Ed., Springer NY, 2015.
2. Yannas I.V., Tzeranis D.S., Mammals fail to regenerate organs when wound contraction drives scar formation. *npj Regen Med* 6, 39 (2021)
3. Hinz B, McCulloch C. A, Coelho N. M., Mechanical regulation of myofibroblast phenoconversion and collagen contraction. *Exp Cell Res* 379, 119-128 (2019).
4. Birk D. E., Trelstad R. L., "Fibroblasts compartmentalize the extracellular space to regulate and facilitate collagen fibril, bundle, and macro-aggregate formation". In A. H. Reddi, Ed., *Extracellular matrix: Structure and function*. (Alan R. Liss. 1985).
5. Ferdman, A. G., Yannas I.V., Scattering of light from histologic sections: A new method for the analysis of connective tissue. *J Invest Dermatol*, 100, 710–716 (1993).
6. Yannas I. V., Lee, E., Orgill D. P., Skrabut E.M., Murphy G.F., Synthesis and characterization of a model extracellular matrix which induces partial regeneration of adult mammalian skin. *Proc Nat. Acad Sci USA* 86, 933–937 (1989).
7. Tzeranis, D. S., Soller, E. C., Buydash, M. C., So, P. T., Yannas I. V., *In situ* quantification of surface chemistry in porous collagen biomaterials. *Ann Biomed Eng* 44, 803–815 (2016).
8. Burke, J. F., Yannas, I. V., Quinby, W. C., Jr., Bondoc, C. C., & Jung, W. K., Successful use of a physiologically acceptable artificial skin in the treatment of extensive burn injury. *Annals of Surgery*, 194, 413–428 (1981).
9. Burke, J. F., Bondoc, C. C., & Quinby, W. C., Primary burn excision and immediate grafting: A method of shortening illness. *The Journal of Trauma*, 14, 389–395 (1974).
10. Heimbach, D., Luterman, A., Burke, J., Cram, A., Herndon, D., Hunt, J., Jordan, M., McManus, W., Solem, L., Warden, G., et al., Artificial dermis for major burns. *Annals of Surgery*, 208, 313–320 (1988).
11. Chang D. K, Louis M. R, Gimenez A, Reece EM., The basics of Integra Dermal Regeneration Template and its expanding clinical applications. *Semin Plast Surg*. 33:185-189 (2019).
12. Opoku-Agyeman, J., Humenansky, K., Davis W. 3rd, Glat, P., Use of Integra for reconstruction after nevi resection: A systematic review and pooled analysis of reported cases, *Surg Res Pract*. 9: 9483627 (2019).
13. Gottlieb, M. E., Furman, J., Successful management and surgical closure of chronic and pathological wounds using Integra®. *Journal of Burns and Surgical Wound Care*, 3, 4 (2004)
14. Prezzavento G.E., Calvi R.N.J., Rodriguez J.A, Taupin P. Integra Dermal Regeneration Template in reconstructive surgery for cutaneous tumors. *J Wound Care*. 31:612-619 (2022).
15. Roels N., Van den Hof B., Integra® Dermal Regeneration Template as an alternative technique to treat degloving injury of fingers. *Acta Chir Belg*. 28:1-3 (2022).
16. Mogedas-Vegara A, Agut-Busquet E, Yébenes Marsal M, Luelmo Aguilar J, Escuder de la Torre Ò. Integra as Firstline Treatment for Scalp Reconstruction in Elderly Patients. *J Oral Maxillofac Surg*. 79:2593-2602 (2021).
17. Hulsen J, Diederich R, Neumeister MW, Bueno RA Jr. Hand (N Y). Integra® dermal

regenerative template application on exposed tendon. 9:539-42 (2014).

18. Piejko M., Radziun K., Bobis-Wozowicz S., Waligórska A., Zimoląg E., Nessler M., Chrapusta A., Madeja Z., Drukała J. Adipose-derived stromal cells seeded on Integra® Dermal Regeneration Template improve post-burn wound reconstruction. *Bioengineering (Basel)*. 7:67(2020).

19. Parshotam K. G., Barker, A., Ahmed, S. et al. Urinary bladder auto augmentation using INTEGRA® and SURGISIS®: an experimental model. *Pediatr Surg Int* 26, 275–280 (2010).